

Atmosphere influence in the pyrolysis of poly[(alkylamino)borazine] for the production of BN fibers

Yongpeng Lei^{a,b,*}, Yingde Wang^{b,*}, Yongcai Song^b

^aCollege of Basic Education for Commanding Officers, National University of Defense Technology, Changsha 410073, PR China

^bScience and Technology on Advanced Ceramic Fibers and Composites Laboratory, College of Aerospace Science and Engineering, National University of Defense Technology, Changsha 410073, PR China

Received 25 December 2012; received in revised form 7 February 2013; accepted 7 February 2013

Available online 13 February 2013

Abstract

The effect of pyrolysis atmosphere on products deriving from poly[(alkylamino)borazine] was studied. Pyrolysis in NH_3 resulted in BN with almost no carbon content while in Ar led to BNC materials. The crystallinity of the sample obtained in NH_3 was higher than that in Ar. BN fibers with almost no carbon impurity were obtained in NH_3 and then in Ar, possessing good oxidation resistance and low dielectric constant. The superior properties of BN fibers allow them to be promising in high-temperature, microwave-transparent applications.

© 2013 Elsevier Ltd and Techna Group S.r.l. All rights reserved.

Keywords: A. Precursors: organic; C. Dielectric properties; E. Functional applications; Fibers

1. Introduction

Due to its superior chemical inertness, high melting point, low density, good oxidation resistance and dielectric constant [1,2], hexagonal boron nitride (*h*-BN) has been studied intensively as advanced ceramic matrix composites in aerospace applications recently [3]. Although BN powder can be easily prepared, it is difficult to fabricate BN in forms of fibers, coatings, porous ceramics and so on. The polymer-derived ceramics route [4], providing nonoxide ceramics with tailored composition and microstructure, has been an attractive method to prepare BN in complex forms [5].

Poly[(alkylamino)borazine]s, possessing B_3N_3 hexagons and plastic alkylamino-units, could be easily processed, heat treated and transformed into BN [6,7]. The carbon in the precursor can be effectively removed during pyrolysis in NH_3 while not in inert atmosphere [8]. As we know, carbon impurity had great impact on the thermal stability in air and

dielectric properties of polymer-derived non-oxide ceramics [9]. But then only limited progress related to pyrolytic carbon in polymer-derived BN has been made [10].

Lately, a novel processable poly[(alkylamino)borazine], poly[2-*n*-propylamino-4,6-bis(methylamino)borazine] (PPAB), has been synthesized from 2,4,6-trichloroborazine (TCB) and *n*-propylamine/methylamine under mild conditions [11]. Here, the effect of atmosphere on the structure, composition and property of pyrolyzed PPAB was researched. Besides, BN fibers with good properties were prepared.

2. Experimental

All samples described here were manipulated in a dry nitrogen atmosphere. The synthesis, spinning and curing of PPAB have been described in Ref. [7,11]. Then, the cured samples were pyrolyzed in Ar and NH_3 at 1000 °C, respectively (heating rate, 4 °C/min. holding time, 1 h). Further heat treatment was achieved at 1800 °C in Ar for 1 h to investigate the crystallization behavior (heating rate, 5 °C/min).

Element contents of N, H and C were checked by Leco TCH-600 N/H/O and Leco CS-600 C/S analyzers. The XPS

*Corresponding author at: National University of Defense Technology, College of Basic Education for Commanding Officers, No.137 Yanwachi Main Street, Changsha 410073, PR China. Tel./fax: +86 731 84575118.

E-mail address: lypkd@yahoo.com.cn (Y. Lei).

spectra were obtained by means of a VG ESCALAB MKII instrument (AlK α excitation). FTIR spectra were recorded on a Nicolet Avatar 360 spectrophotometer as KBr pellets. XRD patterns were obtained using a powder X-ray diffractometer (Siemens D-5005, CuK α radiation). SEM (JSM-6300, JEOL) was used to study the composition of the sample. TGA was conducted on a NETZSCH STA 449C instrument in air (heating rate, 10 °C/min). Density was measured by floatation in halogenated hydrocarbons. HRTEM images were obtained using a Philips CM-200 microscope operated at 200 kV. Raman spectroscopy was carried out using a RM 2000 spectrometer with an argon ion laser at an excitation wavelength of 632.8 nm. The dielectric properties of the powder of sample were determined by the cavity resonator method. The average data were calculated from five tests. The tensile strength was determined from failure tests performed on 30 filaments with a gauge length of 25 mm by using the statistical approach of Weibull [12].

3. Results and discussion

The trend of the weight loss curves of PPAB under Ar and NH $_3$ was similar though the curve obtained in NH $_3$ displayed a lower ceramic yield. At 1000 °C, the ceramic yields in NH $_3$ and Ar were 61.2 and 70.1 wt%, respectively.

The samples pyrolyzed in NH $_3$ and Ar at 1000 °C were named as BN $_a$ and BN $_n$, respectively. The densities of BN $_a$ and BN $_n$ were 1.69 and 1.73 g cm $^{-3}$, lower than the theoretical density of 2.26 g cm $^{-3}$ for *h*-BN. The reason was mainly due to small pores produced during pyrolysis, which was common for polymer-derived ceramics. While the carbon content in BN $_a$ was obviously lower than that in BN $_n$. The difference in carbon content indicated that pyrolysis of PPAB under NH $_3$ resulted in BN with low carbon content, due to the deamination reactions and carbon thermal reduction [13]. While pyrolysis under inert atmosphere led to BNC materials. The sample pyrolyzed in NH $_3$ was gray white while that obtained in Ar was black as a result of the difference in carbon content.

FTIR and Raman spectra give more information on the structural difference (Fig. 1). In Fig. 1a, the C–N bond near 1109 cm $^{-1}$ in BN $_n$ was clear while that was absent in BN $_a$, further suggesting the difference in carbon content. The weak absorption at 3200 cm $^{-1}$ caused by B $_3$ N $_3$ ring opening during pyrolysis was ascribed to N–H in NH $_2$ groups.¹³ While the N–H bond in BN $_a$ was much stronger, indicating the promotion of NH $_3$ to the crosslinking of PPAB. In Fig. 1b, BN $_a$ showed a diffuse peak near 1500 cm $^{-1}$, which is a characteristic of amorphous BN. BN $_n$ displayed two broad graphite carbon peaks attributed to D peak around 1200 cm $^{-1}$ and G peak near 1600 cm $^{-1}$ [14], which were usually found for SiCN and SiBCN containing free carbon [15]. The shift of D peak to lower wavenumber may be due to presence of BN.

XPS analysis was conducted to track the chemical environment of various atoms in two samples (Fig. 2). The signal curves were fitted by peak addition using Gaussian–Lorentzian peak approximations and Shirley background reduction. In the wide scan spectra of both samples, the B1s peak at 190.8 eV and the N1s peak at 397.7 eV confirmed BN [16]. However, the relative intensity of C1s peak in BN $_a$ was much weaker than that in BN $_n$, implying a lower carbon content in BN $_a$. The C1s peak in BN $_n$ can be separated into two peaks attributed to graphite carbon at 284.1 eV [15] and C–N at 285.2 eV [17]. But then the C1s peak in BN $_a$ can only be split into one peak at 284.6 eV assigned to graphite carbon.

Fig. 3a displays the XRD patterns of two samples further heat-treated at 1800 °C in Ar (called BN $_a$ -1800 and BN $_n$ -1800). The peak attributed to (002) plane of *h*-BN was observed for both samples. In BN $_a$ -1800, an obvious peak assigned to the (110) plane and a diffuse hump attributed to the (004) plane were noticed, which were absent in BN $_n$ -1800. Additionally, the full width half maximum of the (002) peak of BN $_a$ -1800 was much narrower than that of BN $_n$ -1800, indicating its relatively higher crystallinity. However, the unsolved (100) and (101) peaks of BN $_a$ -1800 still indicated its turbostratic feature [18]. The XRD

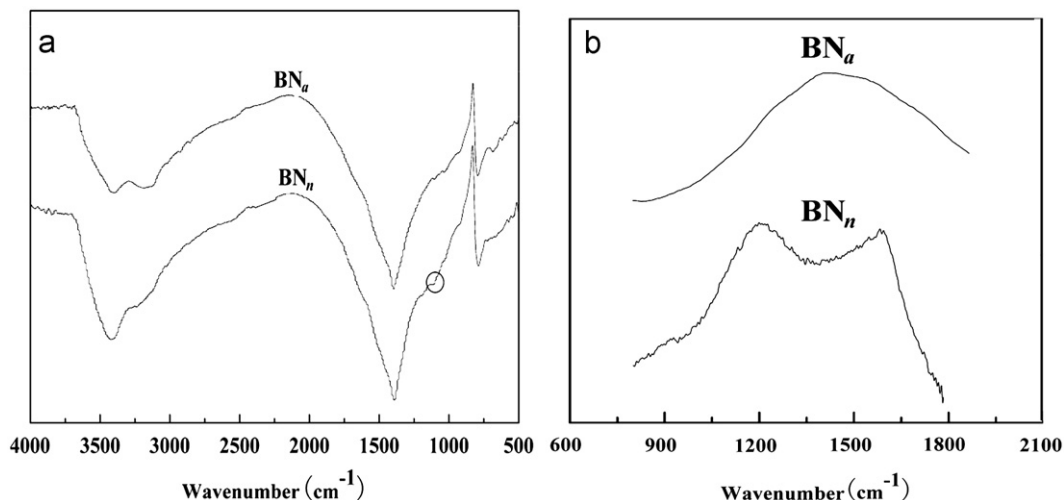


Fig. 1. FTIR and Raman spectra of (a) BN $_n$ and (b) BN $_a$.

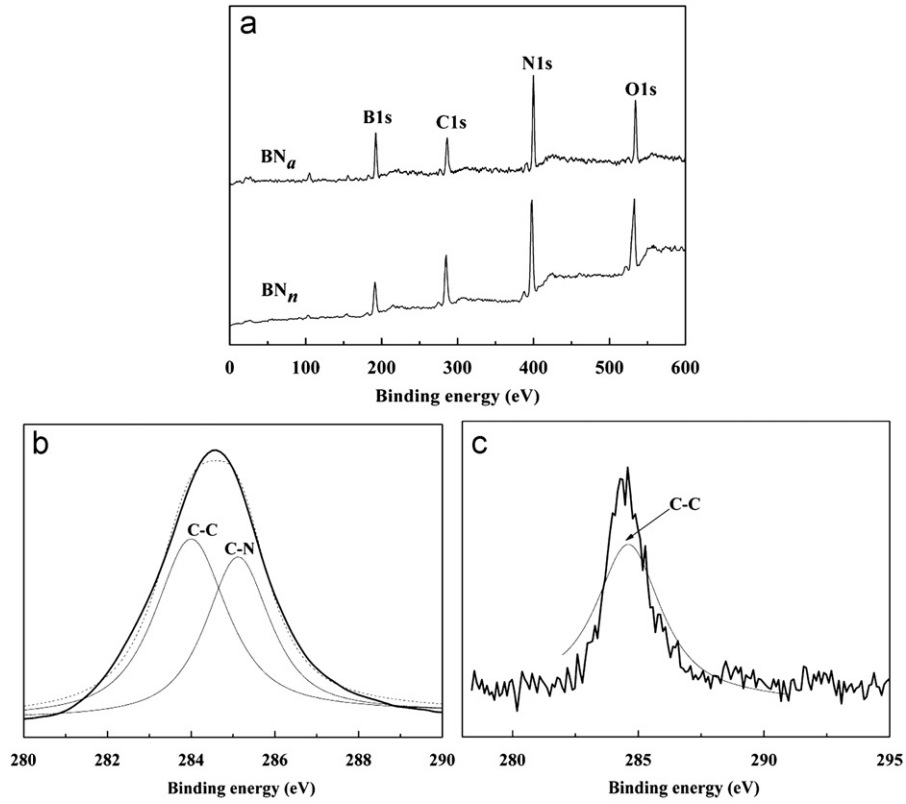


Fig. 2. (a) Wide scan, C1s of (b) BN_n and (c) BN_a XPS spectra.

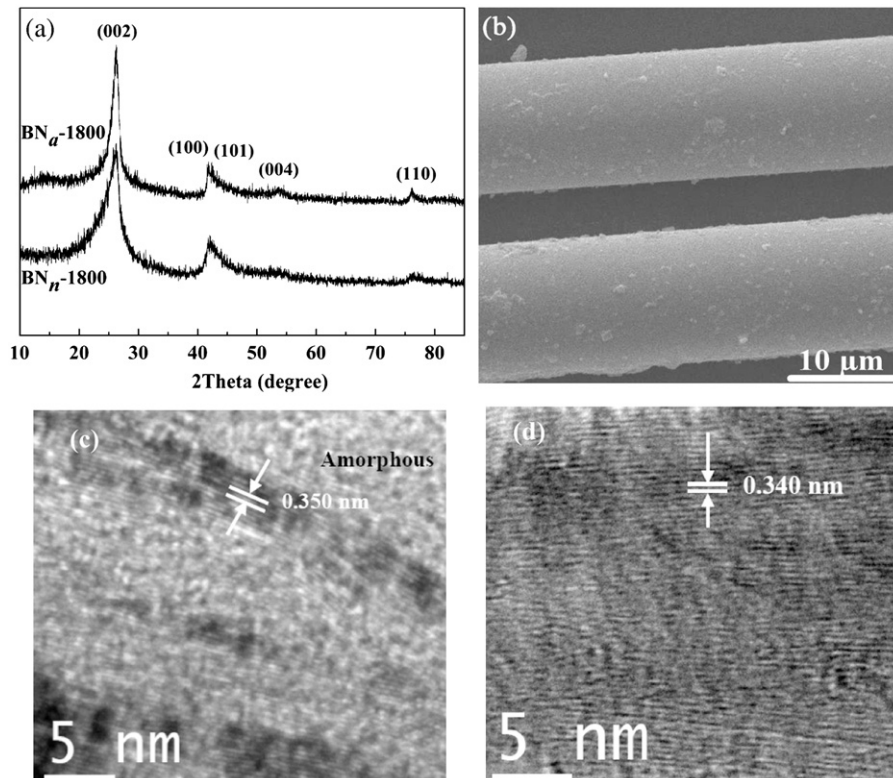


Fig. 3. (a) XRD patterns of two pyrolyzed samples, (b) typical SEM image of BN fiber, TEM images of (c) BN_n-1800 and (b) BN_a-1800 .

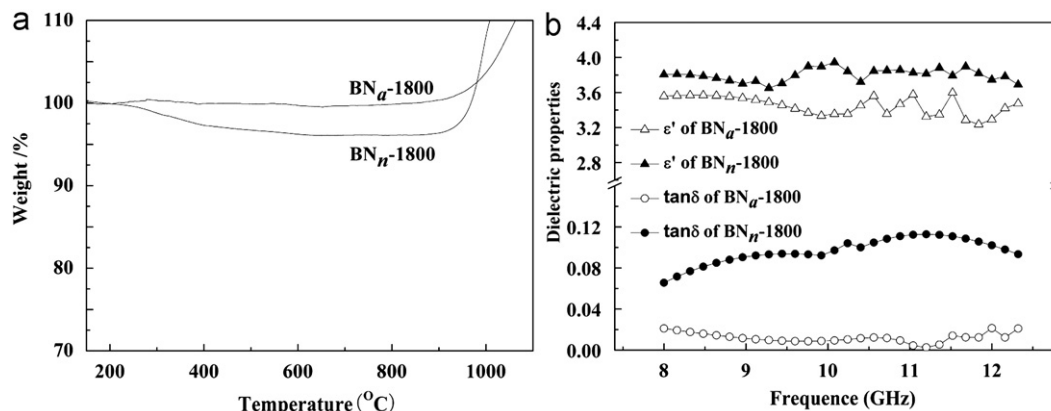


Fig. 4. Oxidation resistance (a) and dielectric properties (b) of two samples.

results showed that pyrolytic carbon favored the stabilization of the ceramic structure against crystallization during pyrolysis [10], just like SiCO and SiCN ceramics [19].

The typical surface SEM image of the BN_a-1800 fiber was given in Fig. 3b. The fiber with a tensile strength of about 0.8 GPa has a smooth surface without any observable flaws though some dust particles were noticed. The tensile strength of the BN fiber pyrolyzed in NH₃ at 1200 °C was only 0.6 GPa, confirming the influence of pyrolysis temperature on the tensile strength of polymer derived fiber [20]. Furthermore, HRTEM was used to further investigate the microstructure (Fig. 3c and d). For BN_n-1800, BN with a poorly-crystallized structure was observed and the interlayer spacing of the (002) plane (d_{002}) was about 0.350 nm. Whereas for BN_a-1800, the d_{002} was 0.340 nm. Hence, the HRTEM result also confirmed the inhibition of pyrolytic carbon on BN's crystallization in BNC, corresponding to the XRD result.

The chemical reactivity of ceramics under special conditions is of crucial importance in determining their applications. Here, the oxidation behavior of two samples was studied in air (Fig. 4). BN_a-1800 displayed excellent oxidation resistance with almost no weight loss until 900 °C (Fig. 4a). But then, for BN_n-1800, the weight loss above 250 °C was due to slow oxidation of carbon [21] and the total weight loss was 3.9 wt% at 900 °C. Therefore, the presence of residual carbon was detrimental to the thermal stability in air. Moreover, both samples showed a weight gain above 900 °C as a result of BN's oxidation [22]. But yet the weight gain of BN_a-1800 was slower than that of BN_n-1800 due to better oxidation resistance. As we know, the sensitivity of BN to oxygen is greatly affected by the crystallinity [23]. Generally, BN possessing higher d_{002} showed higher reaction rates to oxygen, namely more weight gain during oxidation. The BN_a-1800, pyrolyzed from PPAB under NH₃, possessed better thermal stability in air than that pyrolyzed under Ar due to its lower carbon content and higher crystallinity.

Besides good oxidation resistance, composites used in aerospace field, especially the radar-wave-transparent materials, should exhibit low dielectric constant and loss

tangent [24]. Here, the dielectric properties of as-prepared two BN samples were investigated. Fig. 4b reveals the influence of frequency on the dielectric constant (ϵ') and dielectric loss ($\tan \delta$) of two samples. It is clear that both ϵ' and $\tan \delta$ of BN_a-1800 were lower than that of BN_n-1800. The $\epsilon'/\tan \delta$ of BN_a-1800 and BN_n-1800 were 3.32/0.008 and 3.9/0.09 at 10 GHz, respectively. The $\epsilon'/\tan \delta$ of BN_a-1800 at 10 GHz were close to the that of Quartz fiber (3.12/0.0036), which was one of the most commonly used reinforcements in wave-transparent materials [25]. The low carbon content and nearly stoichiometric composition of BN_a-1800 may contribute to the excellent dielectric properties.

4. Conclusions

In conclusion, the effect of pyrolysis atmosphere on the products from PPAB was researched. Pyrolysis in NH₃ resulted in BN with almost no carbon content while in Ar led to BNC materials. In BN_n, carbon existed in form of C–N and C–C bonds while only little carbon stood as graphite in BN_a. The crystallinity of the sample obtained in NH₃ was higher than that in Ar. Finally, the BN fiber prepared in NH₃ then in Ar showed better oxidation resistance and lower dielectric constant/ loss tangent than that in Ar. Combined with its good oxidation resistance and dielectric properties, the BN fiber can be promising for application in high temperature, microwave-transparent system.

Acknowledgments

The National Natural Science Foundation of China (No. 51203182) is acknowledged for financial support.

References

- [1] R.T. Paine, C.K. Narula, Synthetic routes to boron nitride, *Chemical Reviews* 90 (1990) 73–91.
- [2] U. Kusari, Z. Bao, Y. Cai, G. Ahmad, K.H. Sandhage, L.G. Sneddon, Formation of nanostructured, nanocrystalline boron nitride microparticles with diatom-derived 3-D shapes, *Chemical communications* 11 (2007) 1177–1179.

- [3] Y.H. Schlleier, A. Verhoeven, M. Jansen, Observation of direct bonds between carbon and nitrogen in Si–B–N–C ceramic after pyrolysis at 1400 °C, *Angewandte Chemie* 120 (2008) 3656–3658.
- [4] Y.F. Shi, Y. Wan, Y.P. Zhai, R.L. Liu, Y. Meng, B. Tu, D.Y. Zhao, Ordered mesoporous SiOC and SiCN ceramics from atmosphere-assisted in Situ transformation, *Chemistry of Materials* 19 (2007) 1761–1771.
- [5] H. Termoss, B. Toury, S. Pavan, A. Brioude, S. Bernard, D. Cornu, S. Valette, S. Benayoun, P. Miele, Preparation of boron nitride-based coatings on metallic substrates via infrared irradiation of dip-coated polyborazylene, *Journal of Materials Chemistry* 19 (2009) 2671–2674.
- [6] B. Toury, P. Miele, D. Cornu, H. Vincent, J. Bouix, Boron nitride fibers prepared from symmetric and asymmetric alkylaminoborazines, *Advanced Functional Materials* 12 (2002) 228–234.
- [7] Y.P. Lei, Y.D. Wang, Y.C. Song, Y.H. Li, C. Deng, H. Wang, Z.F. Xie, Nearly stoichiometric BN fiber with low dielectric constant derived from poly[(alkylamino)borazine], *Materials Letters* 65 (2011) 157–159.
- [8] P. Dibandjo, L. Bois, F. Chassagneux, D. Cornu, J.M. Letoffe, B. Toury, F. Babonneau, P. Miele, Synthesis of boron nitride with ordered mesostructure, *Advanced Materials* 17 (2005) 571–574.
- [9] R. Vila, M. Gonzalez, M.T. Hernandez, J. Moll, The role of C-impurities in alumina dielectrics, *Journal of the European Ceramic Society* 24 (2004) 1513–1516.
- [10] S. Duperrier, C. Gervais, S. Bernard, D. Cornu, F. Babonneau, P. Miele, Controlling the chemistry, morphology and structure of boron nitride-based ceramic fibers through a comprehensive mechanistic study of the reactivity of spinnable polymers with ammonia, *Journal of Materials Chemistry* 16 (2006) 3126–3138.
- [11] Y.P. Lei, Y.D. Wang, Y.C. Song, Y.H. Li, H. Wang, C. Deng, Z.F. Xie, Facile synthesis of a melt-spinnable polyborazine from asymmetric alkylaminoborazine, *Chinese Chemical Letters* 21 (2010) 1079–1082.
- [12] S.N. Patankar, Weibull distribution as applied to ceramic fibres, *Journal of Materials Science Letters* 10 (1991) 1176–1181.
- [13] S. Bernard, D. Cornu, P. Miele, H. Vincent, J. Bouix, Pyrolysis of poly[2,4,6-tri(methylamino)borazine] and its conversion into BN fibers, *Journal of Organometallic Chemistry* 657 (2002) 91–97.
- [14] X.B. Yan, T. Xu, G. Chen, H.W. Liu, S.R. Yang, Effect of deposition voltage on the microstructure of electrochemically deposited hydrogenated amorphous carbon films, *Carbon* 42 (2004) 3103–3108.
- [15] X.B. Yan, L. Gottardo, S. Bernard, P. Dibandjo, A. Brioude, H. Moutaabbid, P. Miele, Ordered mesoporous silicoboron carbonitride materials via preceramic polymer nanocasting, *Chemistry of Materials* 20 (2008) 6325–6334.
- [16] L. Shi, Y.L. Gu, L.Y. Chen, Y.T. Qian, Z.H. Yang, J.H. Ma, Synthesis and morphology control of nanocrystalline boron nitride, *Journal of Solid State Chemistry* 177 (2004) 721–724.
- [17] J.K. Jeon, Y. Uchamaru, D.P. Kim, Synthesis of novel amorphous boron carbonitride ceramics from the borazine derivative copolymer via hydroboration, *Inorganic Chemistry* 43 (2004) 4796–4798.
- [18] E.J.M. Hamilton, S.E. Dolan, C.M. Mann, H.O. Colijn, C.A. McDonald, S.G. Shore, Preparation of amorphous boron nitride and its conversion to a turbostratic, tubular form, *Science* 260 (1993) 659–661.
- [19] G. Mera, R. Riedel, F. Poli, K. Müller, Carbon-rich SiCN ceramics derived from phenyl-containing poly(silylcarbodiimides), *Journal of the European Ceramic Society* 29 (2009) 2873–2883.
- [20] Y. Kimura, Y. Kubo, N. Hayashi, High-performance boron-nitride fibers from poly(borazine) preceramics, *Composites Science and Technology* 51 (1994) 173–179.
- [21] W.M. Wen, H.N. Xiao, Mechanisms and modeling of oxidation of carbon felt/carbon composites, *Carbon* 45 (2007) 1058–1065.
- [22] Y. Chen, J. Zou, S.J. Campbell, G.L. Caer, Boron nitride nanotubes: pronounced resistance to oxidation, *Applied Physics Letters* 84 (2004) 2430–2432.
- [23] C.G. Cofer, J. Economy, Oxidative and hydrolytic stability of boron nitride—A new approach to improving the oxidation resistance of carbonaceous structures, *Carbon* 33 (1995) 389–395.
- [24] H.J. Wang, J.L. Yu, J. Zhang, D.H. Zhang, Preparation and properties of pressureless-sintered porous Si₃N₄, *Journal of Materials Science* 45 (2010) 3671–3676.
- [25] Y. Tang, J. Wang, X.D. Li, Z.F. Xie, H. Wang, W.H. Li, X.Z. Wang, Polymer-derived SiBN fiber for high-temperature structural/functional applications, *Chemistry—An European Journal* 16 (2010) 6458–6462.